Jason-3 GDR
Quality Assessment Report

Cycle 389

17-09-2024 / 27-09-2024

Prepared by :	B. Flamant , CLS H. Roinard , CLS F. Piras , CLS	
Accepted by :	DT/AQM , CLS	
Approved by :	F. Bignalet-Cazalet , CNES	

CLS
COLLECTE LOCALISATION SATELLITES

SALP
Service Altimetrie & Localisation Precise

SALP-RP-JALT3-EX-23103-CLS389
Edition 01.0, November 2024

1. Introduction

1.1. Document overview

The purpose of this document is to report the major features of the data quality from the Jason-3 mission. The document is associated with data dissemination on a cycle per cycle basis.
This document reports results from Jason-3 GDRs.
The objectives of this document are :

To provide a data quality assessment
To provide users with necessary information for data processing
To report any change likely to impact data quality at any level, from instrument status to software configuration
To present the major useful results for the current cycle

1.2. Software version

The results presented in this report have been performed with GDR products in version F. A detailed description of the products can be found in the Jason-3 user handbook ([1]). This cycle has been produced with the Processing Software references :
L1 library=V5.8, L2 library=V6.10, Processing Pilot=V7.0.3

1.3. Cycle quality and performances

Data quality for this cycle is nominal.

Cycle 389	
Expected number of measurements over ocean	596343
Percentage of missing measurements	0.01 %
Number of available measurements	596256
Percentage of rejected measurements	15.91 %
Rejected due to ice	8.92 %
Rejected with threshold verification (after land and ice removed)	3.84 %
Crossover standard deviation	6.02 cm
Crossover standard deviation on geographical selection [1]	4.70 cm
Sea Level Anomaly standard deviation	11.00 cm
Sea Level Anomaly standard deviation on geographical selection [1]	9.92 cm

TABLE 1: *Summary of cycle 389 performances **over ocean**.*

Analysis of crossovers and sea surface variability indicate that system performances are close to usual values that are obtained from TOPEX/POSEIDON, Jason-1 or Jason-2 data. For this cycle, the crossover standard deviation is 6.02 cm rms. When using a selection to remove shallow waters (1000 m), areas of high ocean variability and high latitudes ($> |50|$ deg.), it decreases down to 4.70 cm rms.

The standard deviation of Sea Level Anomalies (SLA) relative to a 20-year mean is 11.00 cm. When using a selection to remove shallow waters (1000 m), areas of high ocean variability and high latitudes ($> |50|$ deg) it lowers to 9.92 cm .

1. Selection to remove shallow waters (1000 m), areas of high ocean variability and high latitudes ($> |50|$ deg)

— Performances from crossover differences are detailed in the dedicated **section Crossover statistics**.
— Detailed CALVAL results are presented in **section 3**.
— Jason-3 data presented in this report are homogeneous in standard-F over the whole GDR serie
— Note that Jason-3 is on interleaved ground-track from 25-04-2022 11 :00 :00 onwards (cycle 300 pass 159)

1.4. Information about tracking mode

Jason-3 is able to track data with several onboard tracker modes : the Autonomous mode using Median algorithm (also called Median mode) and the Diode/DEM mode. Median mode is similar to the one used by Jason-2. Diode/DEM mode is a technique also used on Jason-2 using information coming from Diode and a digital elevation model available onboard. In addition to Jason-2, Jason-3 Diode/DEM mode has a new option to switch automatically between Diode/DEM mode to Median mode depending on the satellite position. For more information about the different onboard tracker algorithms see [4] (about Jason-2).
Since the last DEM onboard upload (during cycle 168), close loop (“autonomous DIODE acquisition / tracking”) areas are reduced from 23.56% of global measurements to 0.61%.
During this cycle, Jason-3 used Diode/DEM mode.

2. Data coverage and edited measurements

This section presents results that illustrate data quality during this cycle. These verification products are produced operationally so that they allow long term monitoring of missing and edited measurements.

2.1. Missing measurements

This cycle has no missing pass. Missing measurements relative to a nominal ground track are plotted on figure 1.

The map below illustrates missing 1Hz measurements in the GDRs, with respect to a 1 Hz sampling of a nominal repeat track. Missing measurements occur over instrument calibration aeras (over land). Thanks to the upload of an updated OLTC version (add of new inland waters targets) the number of missing measurements over regions with high relief has been significantly reduced since cycle 169 onwards.

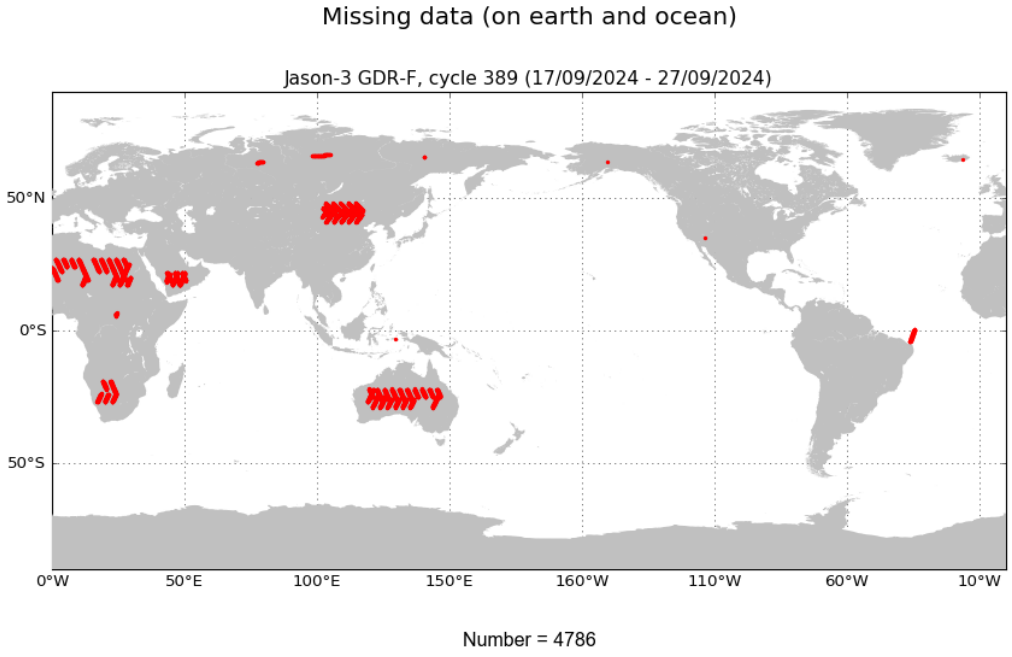

FIGURE 1 – *Missing measurements for cycle 389.*

2.2. Edited measurements

Editing criteria are defined for the GDR product in Jason-3 User Handbook [1].
The editing criteria are defined as minimum and maximum thresholds for various parameters. Measurements are edited if at least one parameter does not lie within those thresholds. These thresholds are expected to remain constant throughout the Jason-3 mission, so that monitoring the number of edited measurements allows a survey of data quality.
The rain flag is not used for data selection.

The number and percentage of points removed over ocean by each criterion is given on the following table. Note that these statistics are obtained with measurements already edited for ice flag (8.92 % of points removed).

Parameters	Min threshold	Max threshold	Unit	Nb removed	% removed
Equilibrium tide	-0.5	0.5	m	0	0.00
Nb measurements of range	10	20	_	5998	1.15
Std. deviation of range	0	0.2	m	7948	1.52
Backscatter coefficient	7	30	dB	3310	0.63
Nb measurements of sigma0	10	20	_	5931	1.14
Std. deviation of sigma0	0	1	dB	12933	2.48
Sea level anomaly	-2	2	m	7930	1.52
Square off nadir angle	-0.2	0.64	deg^2	3443	0.66
Significant wave height	0	11	m	3338	0.64
Altimeter wind speed	0	30	$m.s^{-1}$	6204	1.19
Combined atmospheric correction	-2	2	m	0	0.00
Dry tropospheric correction	-2.5	-1.9	m	0	0.00
Internal tide	-5	5	m	0	0.00
Ionospheric correction filtered	-0.4	0.04	m	4684	0.90
Ocean tide	-5	5	m	34	0.01
Pole tide	-15	15	m	0	0.00
Earth tide	-1	1	m	0	0.00
Sea State Bias	-0.5	0	m	3079	0.59
Sea surface height	-130	100	m	4396	0.84
AMR wet tropospheric correction	-0.5	-0.001	m	566	0.11
Global statistics of edited measurements by thresholds	_	_	_	20048	3.84

TABLE 2: *Table of parameters used for editing.*

The measurements rejected during the editing process are shown in figure 2. Out of over land data, rejected measurements are mainly situated in ice regions and in regions with disturbed sea state.

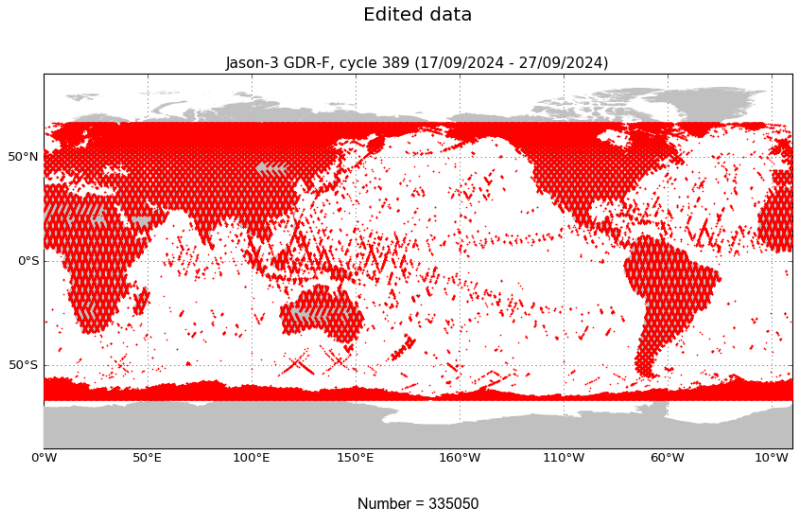

FIGURE 2 – *Edited measurements for cycle 389.*

Map in figure 3 shows the percentage of valid measurements by sample over oceans and seas, with regard to the expected number of points. Wet zones or zones with sea ice appear in the plot as regions with less valid data, as it was also the case for Topex, Poseidon-1, Jason-1 and Jason-2 altimeters : measurements may be corrupted by rain or sea ice. They were therefore removed by editing. As for Jason-2 there are less removed data in these zones and in the areas of strong sea states compared with the usual maps obtained for Topex or Jason-1.

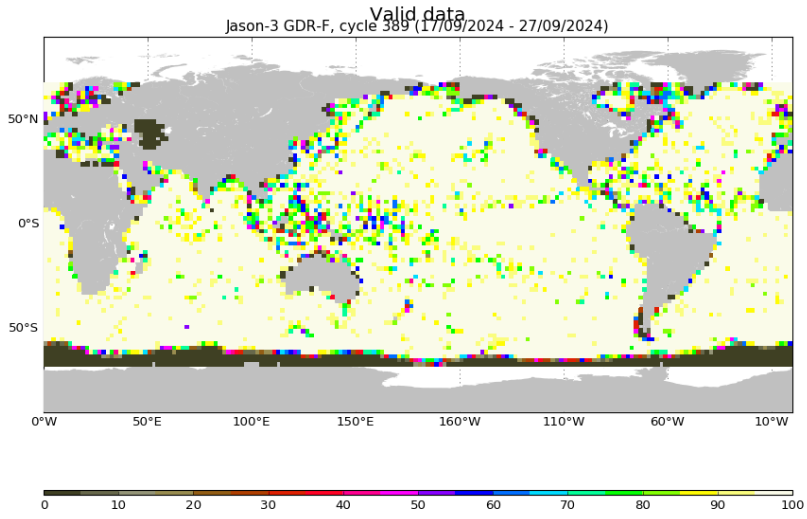

FIGURE 3 – *Percentage of valid measurements for cycle 389.*

3. Instrumental and geophysical parameter analysis

Monitoring of instrumental and geophysical parameters is important in order to detect possible problems. When monitoring parameters over long periods, possible drifts or jumps can be detected. These verification products are produced operationally so that they allow systematic monitoring of the main relevant parameters. When possible, comparison with Jason-2 data are done.

3.1. Jason-3 altimeter and sensor

This section presents the general status of the altimeter for main instrumental variations through the Jason-3 mission. Two calibration modes are used to monitor the altimeter internal drifts and compute the altimetric parameters. They are programmed about three times per day, over land.
The CAL1 mode measures the Point Target Response (PTR) of the altimeter in Ku and C bands. Among the parameters extracted from the PTR are :

— the internal path delay
— the total power of the PTR

The evolutions of these parameters as a function of time are plotted to monitor the ageing of the altimeter.
The CAL2 mode measures the low pass filter of the altimeter in Ku and C bands.

Notice that in the Jason-3 products, the range is corrected for the internal path delay and the backscatter coefficient takes into account the total power of the measured PTR.

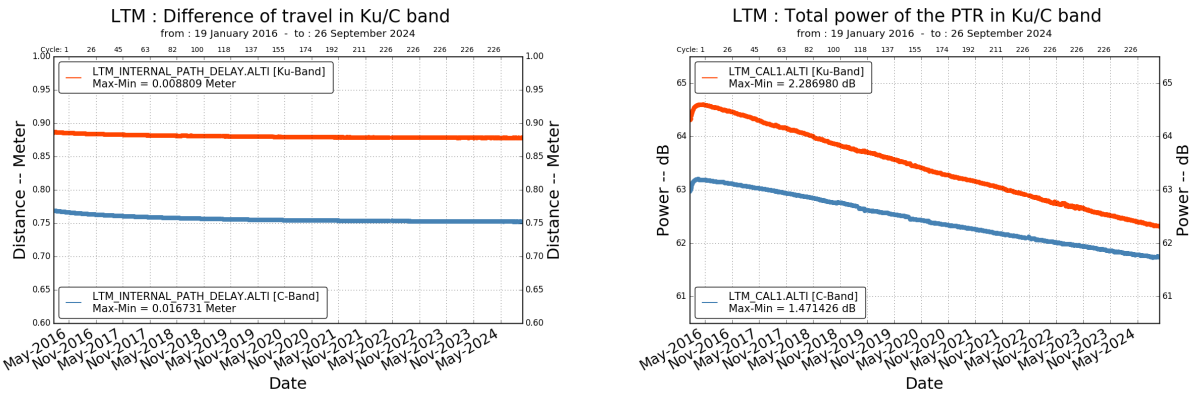

FIGURE 4 – *Internal path delay (left) and total power of the PTR (right) for Ku- and C-band.*

3.2. Significant wave height

Figure 5 shows wave estimations derived from altimeter measurements. Therefore significant wave height data from the current cycle are averaged over a grid of 2° by 2° resolution and smoothed afterwards. Wave height may reach several meters.

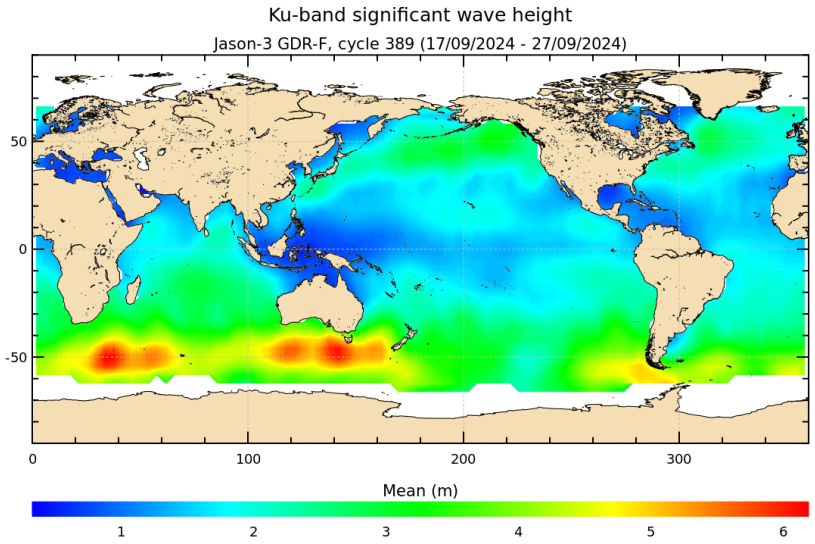

FIGURE 5 – *Significant wave height for cycle 389.*

The daily average of Ku-band SWH for Jason-3 and Jason-2 is plotted as a function of time on left of figure 6. They show similar features.
Normalized histograms over the whole GDR-D serie, 2 years of Jason-3 GDR-F data and over cycle 389 are plotted on the right of the figure. They show similar features, but note that one cycle dispersion median values slightly depends on season time.

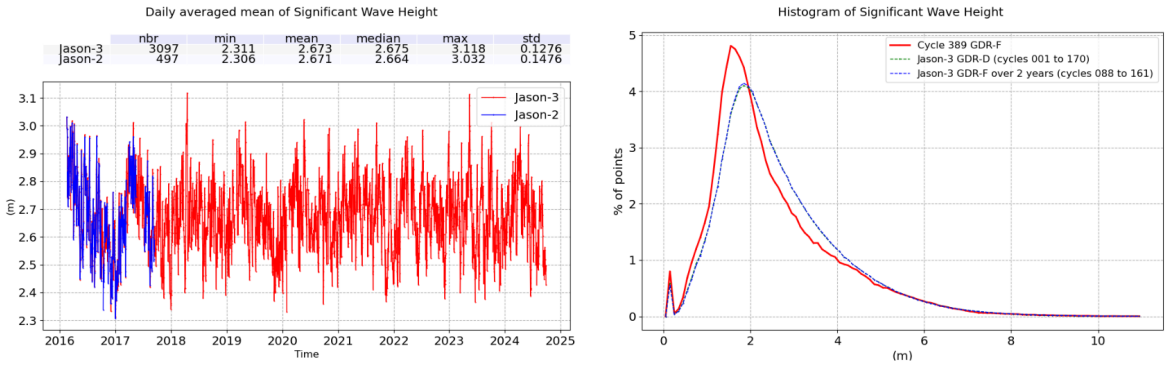

FIGURE 6 – *Daily monitoring of Ku-band significant wave height for Jason-2 and Jason-3 (**left**) and histograms of Jason-3 (**right**).*

3.3. Backscattering coefficient

The daily average of Ku-band backscattering coefficient for Jason-2 and Jason-3 is plotted as a function of time on left of figure 7. Beside a bias of about 0.22 dB between Jason-3 GDR-F and Jason-2 GDR-D (determined during the verification phase of Jason-3), they show similar features.

Normalized histograms over the whole GDR-D serie, 2 years of Jason-3 GDR-F data and over cycle 389 are plotted on the right of the figure. They show similar features.

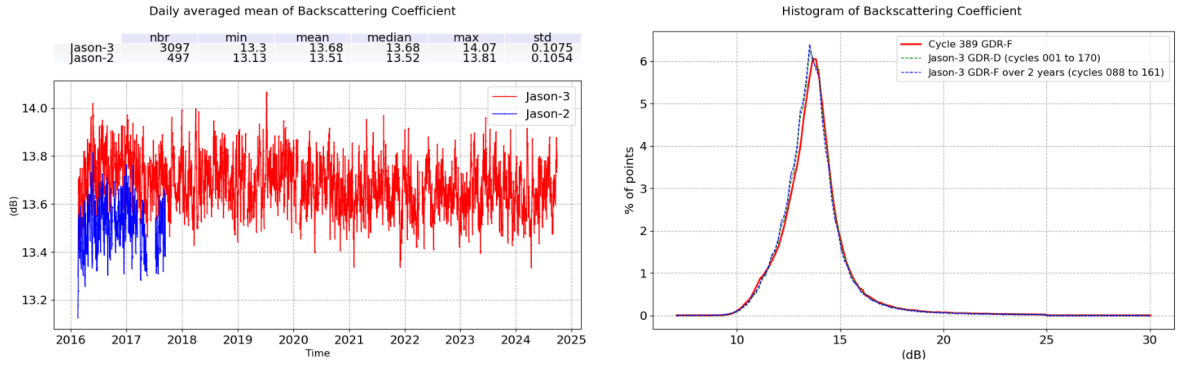

FIGURE 7 – *Daily monitoring of Ku-band backscattering coefficient for Jason-2 and Jason-3 (**left**) and histograms of Jason-3 (**right**).*

3.4. Dual frequency ionosphere correction

The daily average of dual-frequency ionosphere correction for Jason-3 and Jason-2 is plotted as a function of time on left of figure 8. They show similar features, but a bias of about 9.0 mm is visible (value computed for Jason-3 minus Jason-2 over the tandem phase). This bias comes from Ku and C-band range and SSB differences between Jason-3 and Jason-2.

Normalized histograms over the whole GDR-D serie, 2 years of Jason-3 GDR-F data and over cycle 389 are plotted on the right of the figure.
Due to the start of a 25th cycle, the solar activity began increasing in 2020 (and will be at a maximum round mid-2025 following the NOAA Space Weather Prediction Center predictions [5]). This is visible on the ionospheric correction deduced from altimeter measurements increase on the left of figure 8. This correction is slightly higher for the current cycle compared to previous periods on the right of figure 8.

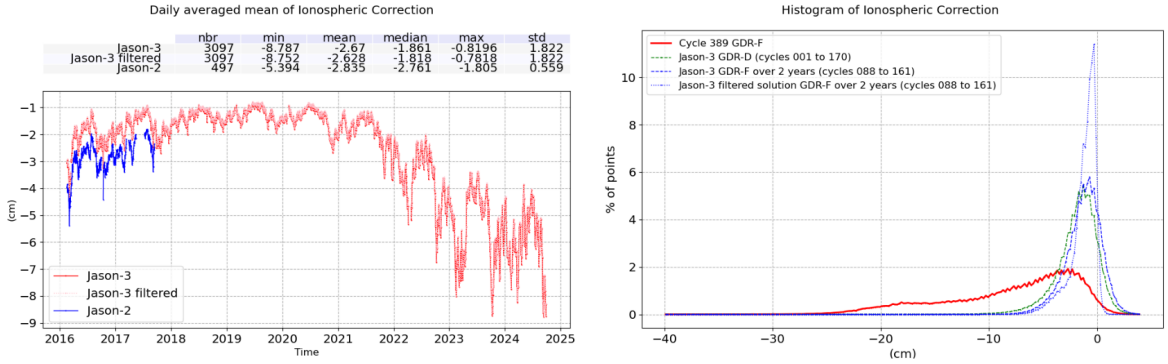

FIGURE 8 – *Daily monitoring of dual-frequency ionosphere correction for Jason-2 and Jason-3 (**left**) and histograms of Jason-3 (**right**).*

3.5. Altimeter wind speed

Figure 9 shows altimeter wind estimations derived from altimeter measurements. Therefore the data from the current cycle are averaged over a grid of 2° by 2° resolution and smoothed afterwards.

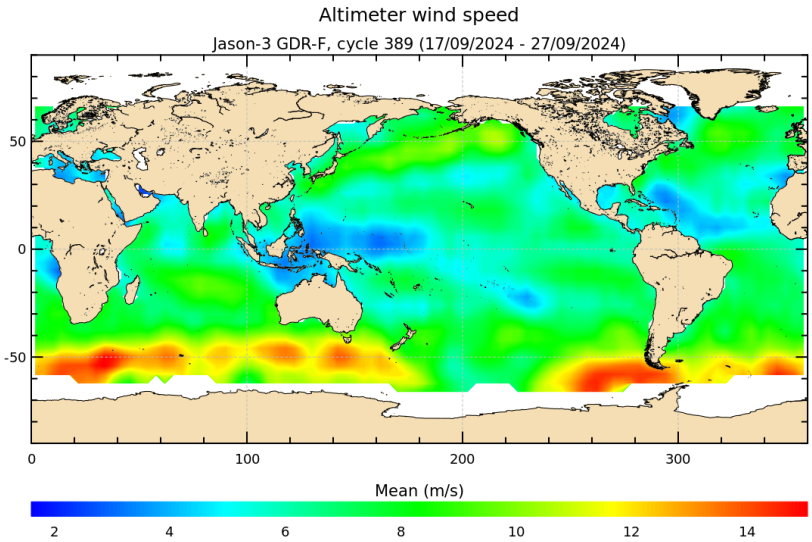

FIGURE 9 – *Altimeter wind speed for cycle 389.*

The daily average of altimeter wind speed for Jason-3 and Jason-2 is plotted as a function of time on left of figure 10. Since 16-03-2016 (platform pointing change, impacting sigma0 and so wind speed), a small bias has been visible between Jason-2 and Jason-3. Except this bias, they show similar features, and the Jason-3 minus Jason-2 bias between the two missions is around 0.1 m/s.
Normalized histograms over the whole GDR-D serie, 2 years of Jason-3 GDR-F data and over cycle 389 are plotted on the right of the figure.
Jason-3 GDR-F wind speed differs from GDR-D and is now closer to ERA5 model (+0.4m/s bias, see change in distribution on right of figure 10).

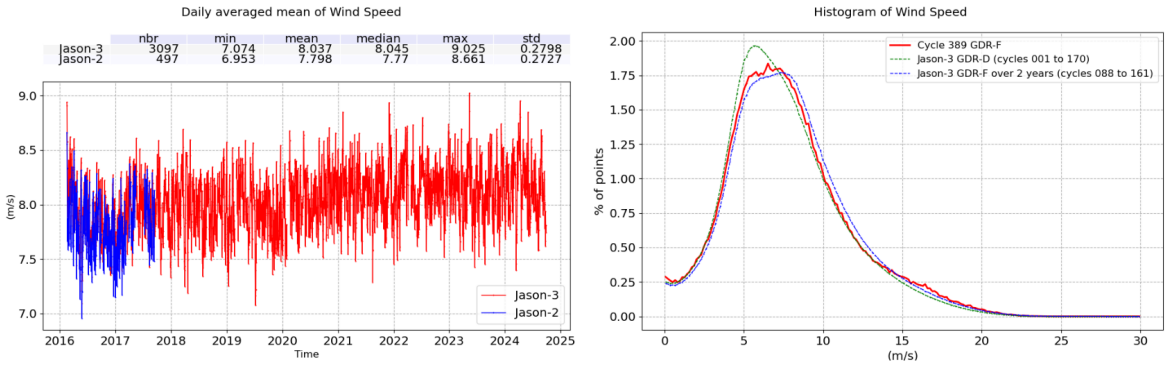

FIGURE 10 – *Daily monitoring of altimeter wind speed for Jason-2 and Jason-3 (**left**) and histograms of Jason-3 (**right**).*

3.6. Radiometer parameters

Figure 11 shows the mean and standard deviation of wet troposphere correction (radiometer - ECMWF) difference by pass for current cycle. Beside natural pass to pass variations, there is no anomaly detectable.

The daily average of wet troposphere correction (radiometer - ECMWF) difference for Jason-3 and Jason-2 is plotted as a function of time on left of figure 12. Normalized histograms over the whole GDR-D serie, 2 years of Jason-3 GDR-F data and over cycle 389 are plotted on the right of the figure. They show similar features around their means. There is a bias of -6.3mm from Jason-3 GDR-D to GDR-F wet troposphere correction (radiometre - model) difference.

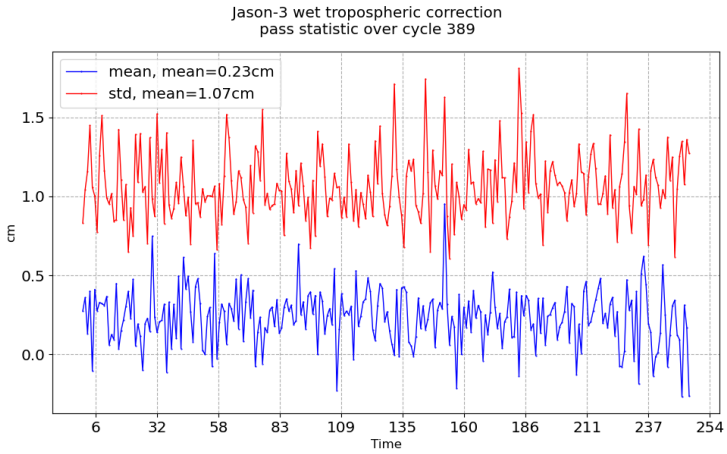

FIGURE 11 – *Pass monitoring of wet troposphere differences between radiometer and ECMWF model for Jason-3 cycle 389*

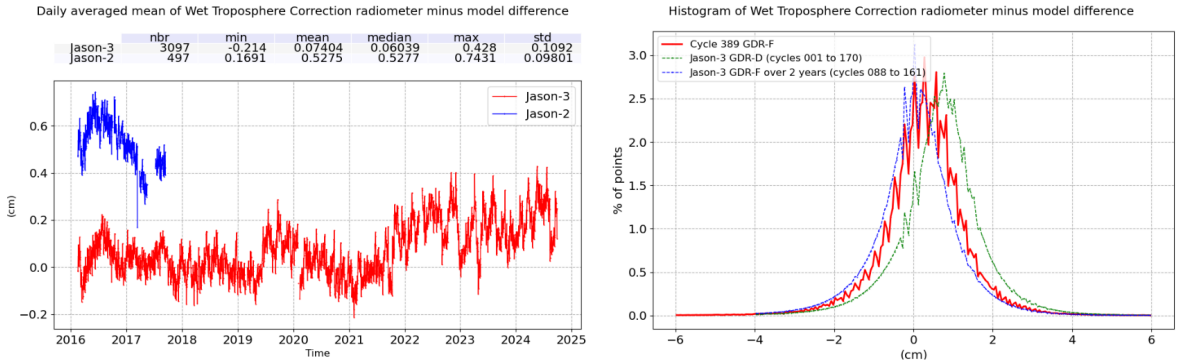

FIGURE 12 – *Daily monitoring of wet troposphere differences between radiometer and ECMWF model for Jason-2 and Jason-3 (**left**) and histograms of Jason-3 (**right**).*

For Jason-3 as for Jason-2, an Autonomous Radiometer Calibration System (ARCS) is used prior to GDR production for the Jason-3 radiometer (AMR) in order to monitor calibrations and recalibrate if necessary (for more details see [3] dealing with Jason-2 system). The plot of daily means of (Radiometer - ECMWF) wet troposphere correction was quite stable, even though ARCS does not use the ECMWF model to calibrate the AMR. Nevertheless small variations of up to 2 mm amplitude are observable. They can be due to (among others) evolution of ECMWF model (for example on June 2019 with +1mm due to changes in ECMWF model) or ARCS calibrations.

Jumps can occur on the radiometer wet tropopshere correction due to Safe Hold Modes (SHM). *(Jason-2 encountered SHM from the 15/03/2017 to the 30/03/2017, from the 17/05/2017 to the 11/07/2017 and from the 14/09/2017 to 13/10/2017. Jason-3 encountered SHM from the 24/02/2019 to the 06/03/2019, from the 06/04/2019 to the 12/04/2019, from the 31/01/2020 to 13/02/2020 and from the 15/06/2020 to the 19/06/2020.)*

Note that Jason-3 AMR have been recalibrated about every 2 months with cold sky calibration until mid-2017 and then every 30 days in average.

Though for GDR, the drifts and jumps are approximatively corrected by ARCS (by discrete values), drifts are still visible within a cycle. Furthermore, the application of a discrete recalibration can also lead to jumps in the time series.

4. Crossover Analysis

4.1. Overview

SSH crossover differences are the SSH differences between ascending and descending passes where they cross each other. Crossover differences are systematically analyzed to estimate data quality and the Sea Surface Height (SSH) performances. SSH crossover differences are computed from the valid data set on a one cycle basis, with a maximum time lag of 10 days, in order to limit the effects of ocean variability which are a source of error in the performance estimation. The mean SSH crossover differences should ideally be close to zero and standard deviation should ideally be small.

Nevertheless SLA varies also within 10 days, especially in high variablity areas. Furthermore, due to lower data availability (due to seasonal sea ice coverage), models of several geophysical corrections are less precise in high latitude. Therefore an additional geographical selection - removing shallow waters, areas of high ocean variability and high latitudes ($> |50|$ deg) - is applied for cyclic monitoring.

4.2. Maps of SSH crossover differences

After data editing, applying additional geographical selection and using the standard Jason-3 algorithms, the crossover standard deviation is about 4.70 cm rms.
The map of the mean differences at crossovers (4 by 4 degrees by bins) is plotted for the current cycle on left panel of figure 13, whereas the right panel shows the whole Jason-3 period.

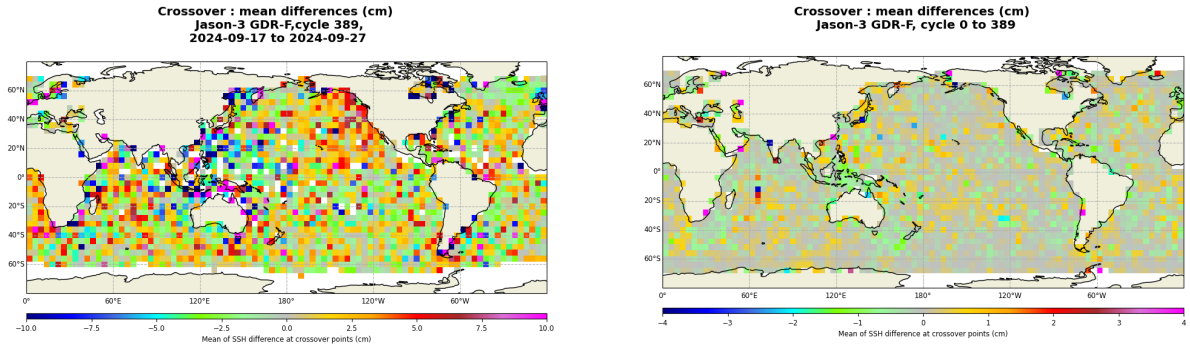

FIGURE 13 – *Mean SSH at crossovers for cycle 389 (left) and over the whole Jason-3 period (right).*

4.3. Cycle by cycle monitoring

The mean and standard deviation of SSH differences at crossovers are plotted for Jason-3 and Jason-2 as a function of time on a one cycle per cycle basis in figure 14. Note that cycle 001 of Jason-3 corresponds to cycle 281 of Jason-2. The statistics are computed after data editing and using the geographical selection criteria.
A 120-days signal seems to appear on Jason-3 SSH differences at crossover (significantly reduced compared to GDR-D thanks to POE-F).

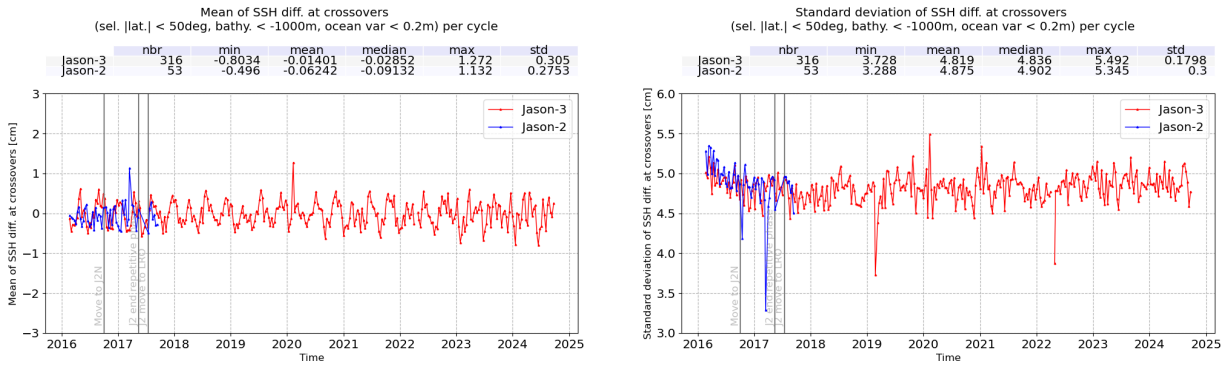

FIGURE 14 – *Cyclic monitoring of mean (left) and standard deviation (right) of SSH differences at crossovers for Jason-3 and Jason-2.*

Figure 15 shows the mean and the standard deviation of Jason-2 − Jason-3 10-day SSH crossovers, using radiometer wet troposphere correction for both satellites or ECMWF model wet troposphere correction. Note that Jason-2 corrections are updated as much as possible to be in line with Jason-3 GDR-F standards (POE-F orbit standard, Tran2018 SSB and deduced filtered ionospheric correction, ocean tide, internal tide, pole tide).

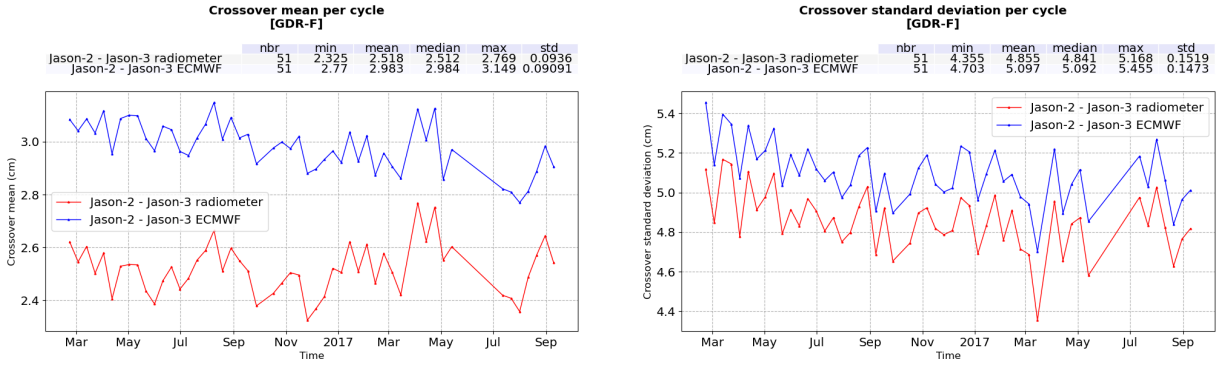

FIGURE 15 – *Cyclic monitoring of mean (left) and standard deviation (right) of (Jason-2 − Jason-3) SSH differences at crossovers.*

4.4. Comparison of pseudo time tag bias

The pseudo time tag bias is found by computing at SSH crossovers a regression between SSH and orbital altitude rate ($\dot{H}$), also called satellite radial speed :

$$SSH = \alpha \dot{H}$$

This method allows us to estimate the time tag bias but it absorbs also other errors correlated with $\dot{H}$ as for instance orbit errors. Therefore it is called "pseudo" time tag bias.

The monitoring of this coefficient estimated at each cycle is performed for Jason-3 and Jason-2 in the following figure : it hightlights that pseudo time tag bias is close to zero (mean value) for both missions.

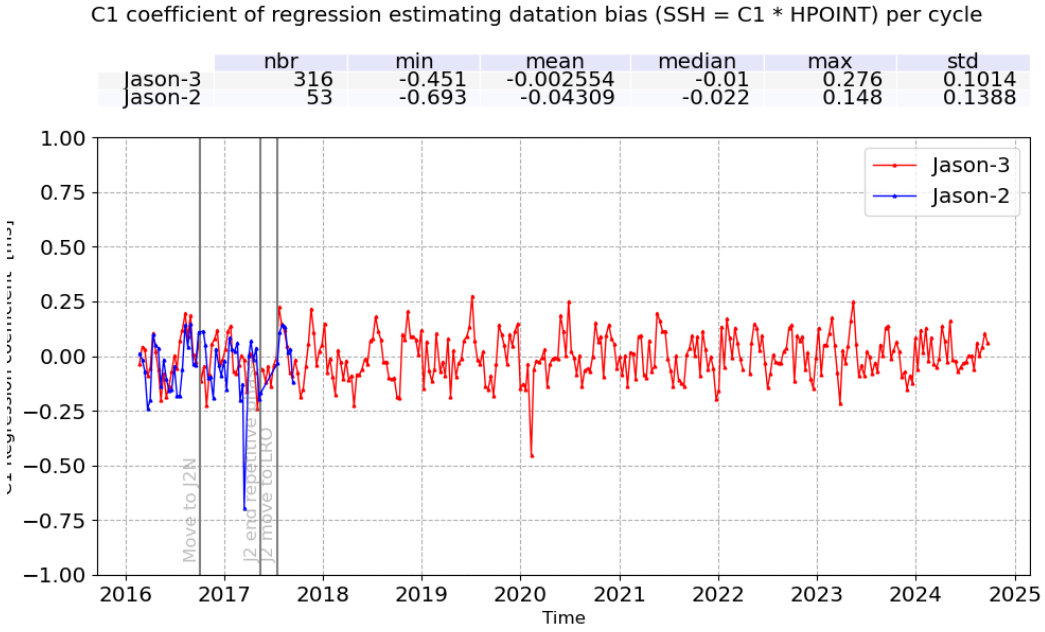

FIGURE 16 – *Cyclic monitoring of pseudo time tag bias for Jason-3 and Jason-2.*

5. Along track analysis

5.1. Mean of along-track SLA

5.1.1. Temporal analysis

The monitoring of mean SLA for Jason-3 and Jason-2 (Figure 17 on left) and the monitoring of mean SLA differences between both missions (Figure 17 on right) show a very stable bias (close to 3.0 cm).

Note that during the Jason-3/Jason-2 tandem phase (Cycles 1 to 23), the SSH bias estimation is performed very accurately (0.1 cm). This allows us to link together Jason-3 and Jason-2 MSL time data series (see section **Mean Sea Level estimations**).

Note that Jason-2 corrections are updated as much as possible to be in line with Jason-3 GDR-F standards (POE-F orbit standard, Tran2018 SSB and deduced filtered ionospheric correction, ocean tide, internal tide, pole tide, mss).

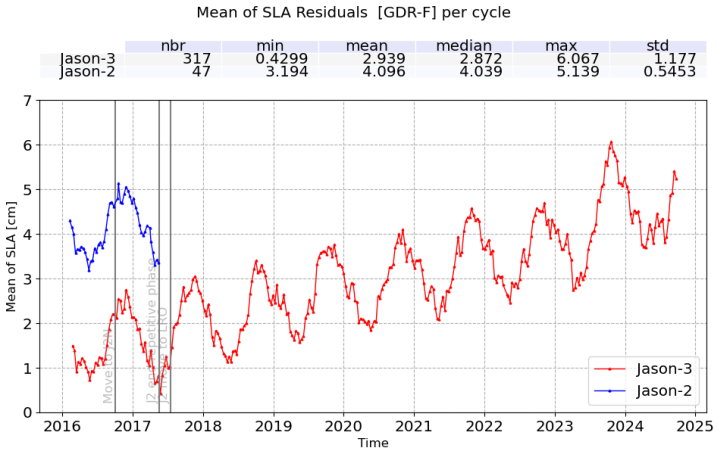

FIGURE 17 – *Cyclic monitoring of mean SLA for Jason-3 and Jason-2.*

5.1.2. Maps

Figure 18 show the map of Jason-3 SLA relative to the MSS.

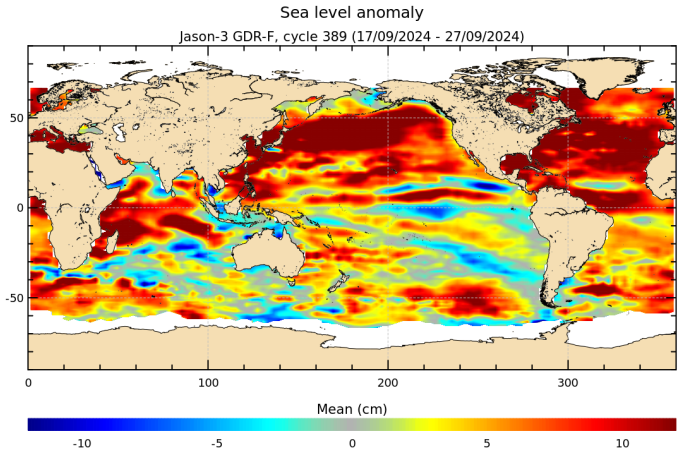

FIGURE 18 – *Sea level anomaly relative to MSS for cycle 389.*

Since Jason-2 has moved to its new interleaved orbit, maps of direct Jason-2 − Jason-3 SLA measurements are no longer available. But differences of gridded SLA for Jason-2 and Jason-3 can be made. This difference is quite noisy for one cycle, especially as **both satellites are shifted in time and sea state changes especially in regions of high ocean variability**. Therefore left panel of figure 19 shows an average over SLA grid differences from several cycles (over cycle 025 to cycle 058). High variability regions as Gulf Stream and Antarctic circumpolar current are visible. On right panel of figure 19, colocated Jason-2 − Jason-3 SLA differences averaged over the period of tandem phase (cycle 001 to 023) are shown. Note that Jason-2 corrections are here updated as much as possible to be in line with Jason-3 GDR-F standards (POE-F orbit standard, Tran2018 SSB and deduced filtered ionospheric correction, ocean tide, internal tide, pole tide, mss). **As both satellites measure the same oceanic features only 1'20" apart, only a weak hemispheric bias is visible (likely due to differences in orbit processing).**

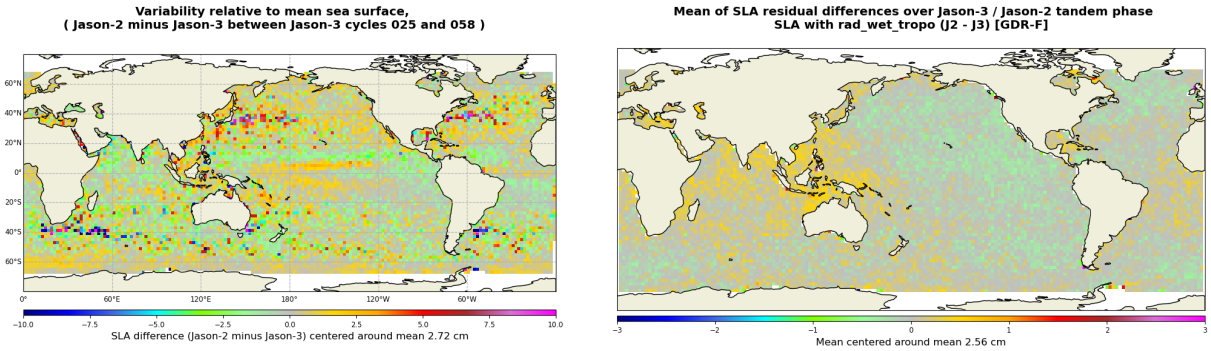

FIGURE 19 – *Jason-2 − Jason-3 SLA differences averaged over Jason-3 period from cycle 025 until cycle 058 (left), and for tandem phase (cycle 001 to 023) (right).*

5.2. Along-track performances

Sea Level Anomaly (SLA) statistics are computed from repeat-track analysis. The plot below gives the standard deviation of the SLA for each cycle over the whole data set. Note that Jason-2 corrections are here updated as much as possible to be in line with Jason-3 GDR-F standards (POE-F orbit standard, Tran2018 SSB and deduced filtered ionospheric correction, ocean tide, internal tide, pole tide, mss).
There are no values for Jason-2 during Jason-3 cycle 24 and half of cycle 25 (corresponding to Jason-2 cycles 304 and 305) because the Jason-2 satellite is moved to the flight formation orbit on the new ground track. This was already the ground track of TOPEX during its formation flight with Jason-1, and Jason-1 with Jason-2. In addition, Jason-2 is temporally shifted by 5 days.

Jason-2 encountered Safe Hold Modes from the 15/03/2017 to the 30/03/2017, from the 17/05/2017 to the 11/07/2017 and from the 14/09/2017 to the 13/10/2017, so that Jason-2 measurements are missing. Jason-3 encountered Safe Hold Modes from the 24/02/2019 to the 06/03/2019, from the 06/04/2019 to the 12/04/2019, from the 31/01/2020 to 13/02/2020 and from the 15/06/2020 to the 19/06/2020, so that Jason-3 measurements are missing. Note that cyclic statistics can be different over such cycles due to uncomplete global coverage.

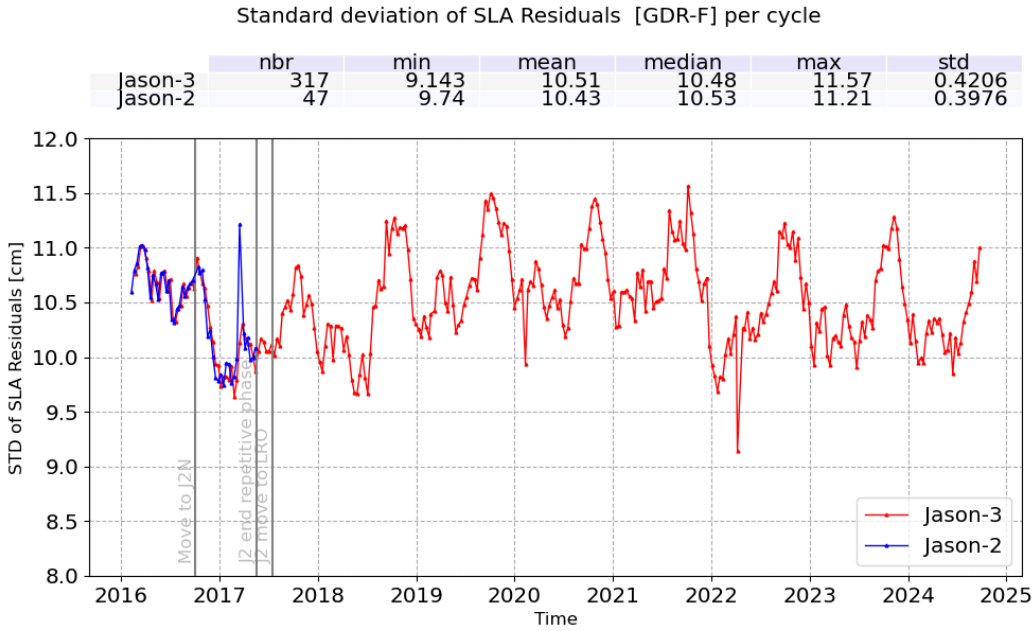

FIGURE 20 – *Cyclic monitoring standard deviation of along track SLA for Jason-3 and Jason-2.*

6. Mean Sea Level estimations (MSL)

6.1. Global MSL trend

Over the tandem phase of Jason-3 (till cycle 023), both Jason-2 and Jason-3 satellites flew on the same ground track, only 1mn20s apart. They therefore measured the same features, allowing to calibrate Jason-3. This allowed to link precisely the MSL time series of Jason-2 and Jason-3. The uncertainty of the bias value between the two time series is less than 1 mm. The evolution of the ocean mean sea level can therefore be precisely observed on a continual basis since 1993 thanks to the 4 reference missions : TOPEX/Poseidon, Jason-1 (from may 2002 to october 2008), Jason-2 (from october 2008 to may 2016) and now Jason-3 (since june 2016).

Wet troposphere correction, inverse barometer correction, GIA (-0.3 mm/yr) are applied to calculate the MSL and the data series are linked together accurately thanks to the tandem flying phases. The following global bias are applied : -2.260 cm between T/P&Jason-1, 3.900 cm between Jason-1/Jason-2 and 2.880 cm between Jason-2/Jason-3. An exhaustive overview over possible errors impacting the MSL evolution is given in [2].
Furthermore, annual and semi-annual signals are removed from the time serie and a 2-month filter is applied. For more details, see MSL Aviso Website : http://www.aviso.altimetry.fr/msl.

6.2. Regional MSL trends

Though mean sea level trend is globally positive, it is inhomogeneous distributed over the ocean. Locally, sea level rise or decline up to ± 10 mm/yr are observed on right panel of figure 21. The map of regional MSL trends is estimated from multi-mission grids (Ssalto/DUACS products) in order to improve spatial resolution. Data from Jason-3 mission were introduced in DUACS system end of September 2016 (when Jason-2 moved to its new interleaved orbit).

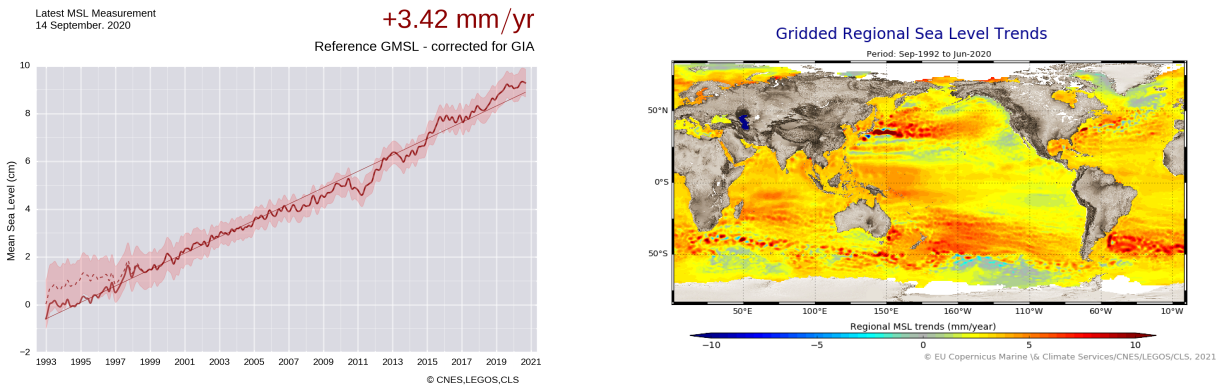

FIGURE 21 – *Global (left) and regional (right) MSL trends from 1993 onwards.*

Références

[1] Jason-3 Products Handbook, GDR-F version, June 2021 *SALP-MU-M-OP-16118-CN*. Available at : https://www.aviso.altimetry.fr/fileadmin/documents/data/tools/6ddbb265-147f-4086-9a2b-8d15989219ec.pdf

[2] M. Ablain, Cazenave, A., Valladeau, G., and Guinehut, S. 2009 : A new assessment of the error budget of global mean sea level rate estimated by satellite altimetry over 1993-2008. *Ocean Sci,* **5,** 193-201. Available at http://www.ocean-sci.net/5/193/2009/os-5-193-2009.pdf *Ocean Sci,* **5,** 193-201. Available at http://www.ocean-sci.net/5/193/2009/os-5-193-2009.pdf

[3] S. Brown, S. Desai, W. Lu, and A. Sibthorpe. 2009 : Performance assessment of the Advanced Microwave radiometer after 1 year in Orbit. *OSTST Seattle, USA,*. Available at : www.aviso.altimetry.fr/fileadmin/documents/OSTST/2009/oral/Brown.pdf

[4] J.-D. Desjonqueres, G. Carayon, J.-L. Courriere, and N. Steunou, 2008. Poseidon 3 In-flight results. *OSTST Nice, France*. Available at : www.aviso.altimetry.fr/fileadmin/documents/OSTST/2008/oral/desjonqueres.pdf

[5] Space Weather Prediction Center. National Oceanic and Atmospheric Administration. Solar cycle progression https://www.swpc.noaa.gov/products/solar-cycle-progression